CHALMERS
UNIVERSITY OF TECHNOLOGY

Influence of electrical conductivity on the electroosmotic dewatering of cellulose nanocrystals

Master's Thesis in Innovative and Sustainable Chemical Engineering

Erik Kullberg

Department of Chemistry and Chemical Engineering
CHALMERS UNIVERISTY OF TECHNOLOGY
GOTHENBURG, SWEDEN, 2018

Master's Thesis 2018

Influence of electrical conductivity on the electroosmotic dewatering of cellulose nanocrystals

Erik Kullberg

Department of Chemistry and Chemical Engineering
Division of Forest Products and Chemical Engineering
CHALMERS UNIVERSITY OF TECHNOLOGY
Gothenburg, Sweden 2018

Influence of electrical conductivity of the electroosmotic dewatering of cellulose nanocrystals

Erik Kullberg

Supervisors: Jonas Wetterling, Department of Chemistry and Chemical Engineering

Tuve Mattsson, Department of Chemistry and Chemical Engineering

Examiner: Professor Hans Theliander, Department of Chemistry and Chemical Engineering

Master's Thesis 2018

Department of Chemistry and Chemical Engineering

Division of Forest Products and Chemical Engineering

Chalmers University of Technology

SE-412 96 Gothenburg

Telephone +46 31 772 1000

Gothenburg 2018

Acknowledgments

The work that have been done during this master thesis would not have been possible without all the invaluable help that has been given from all persons at the division of forest products and chemical engineering at Chalmers. I would also like to give a special thanks to a few persons.

Professor Hans Theliander, examiner, for his help and interest in the project.

Jonas Wetterling, supervisor, for his support, help, guidance and expertise over the entire project.

Karin Sahlin, for all the help with production of cellulose nanocrystals and characterization of the cellulose nanocrystals.

Tuve Mattsson, co supervisor, for his support and interest in the project.

Anders Mårtensson, for his help with AFM pictures during the characterization.

Abstract

Cellulose nanocrystals (CNC) is a renewable material derived from trees which has the potential to be used in a wide variety of materials in the future. It has high crystallinity and at least one dimension in the nanometer range. One main issue with the production of the cellulose nanocrystals on large scale is to obtain an energy-efficient dewatering. However, recent studies have shown that electroosmotic dewatering is a possible dewatering alternative. This operation is strongly dependent of the electrical conductivity of the suspension of the cellulose nanocrystals, which was the main focus of this investigation.

The production of the cellulose nanocrystals was done through acid hydrolysis followed by dialysis to remove excess acid. The suspensions of cellulose nanocrystals were removed at different points in the dialysis giving different conductivity levels of the cellulose suspensions. Then the suspensions containing cellulose nanocrystals were dispersed through sonication.

The electroosmotic dewatering of the cellulose nanocrystals was carried out in a filter cell with two platinum electrodes which an electric field was applied over. The electric field was applied with either constant current or constant voltage. The electroosmotic dewatering behavior were analyzed at the different conductivity levels from the dialysis to see the influence of the electrical conductivity on the electroosmotic dewatering behavior. The dewatering experiments showed more favorable characteristics in the regard of a lower energy demand and a higher dewatering rate for suspensions with lower electrical conductivity. Additionally, if the electrical conductivity of the suspensions was too high it was not possible to perform dewatering this way without damaging the cellulose nanocrystals through pyrolysis reactions. Experiments performed with constant applied voltage showed a more stable dewatering behavior.

The influence of pH adjustment on the electroosmotic dewatering of the suspensions of cellulose nanocrystals were also investigated. The suspensions were dewatered at their original conditions or adjusted to pH 5 before the dewatering. The pH adjusted suspensions gave a small decrease in energy demand compared to the dewatering experiments without pH adjustment. However, the energy demand for all experiments where no pyrolysis occurred, regardless if dewatering were performed at constant applied current, constant applied voltage or with any pH adjustment, were able to effectively lower the energy demand compared to drying.

Keywords: Cellulose nanocrystals, electroosmotic dewatering, electrical conductivity

Contents

1 Introduction

1.1 Background

During the last century the consumption of fossil based products have increased drastically. Since these products are not sustainable to use in a long term perspective new renewable options are being considered to utilize in the production of materials and fuels (Ragauskas et al., 2006).

Cellulose nanocrystals is a material of growing interest as a potential source of bio-based materials. The advantages with using cellulose nanocrystals is that they are both renewable and biodegradable and have a number of favorable characteristics such as good optical properties, high surface area and excellent mechanical strength (Peng et al., 2011). These properties makes it useful for production of films, foams and nanocomposites (Abitbol et al., 2016).

One way to produce cellulose nanocrystals is through acid hydrolysis of cellulose fibers followed by dialysis to remove the excess acid and then dispersion of the cellulose nanocrystals. Thereafter post-treatment consisting of purification and fractioning may be used to increase the quality of the cellulose nanocrystals (Dufresne, 2012). Cellulose nanocrystals may also be modified to fit the product better, for example by making the surface hydrophobic for packaging materials (Abitbol et al., 2016). Before use of the cellulose nanocrystals the suspensions have to be dewatered from the dilute conditions after the acid hydrolysis and dialysis. This process is often very energy demanding as mechanical dewatering is hindered by the large surface area of cellulose nanocrystals. The use of more energy intensive dewatering operations such as thermal drying could therefore have a substantial influence on the process economy.

To obtain an energy-efficient dewatering is important both from an economical point of view as well as for the environmental impact of the production. One promising way is electro-assisted filtration which has been shown to increase the dewatering rate compared to pressure filtration for materials with high surface area such as gelatinous sludge and vegetable sludge (Mahmoud et al., 2010). The technology has also shown potential for cellulose nanocrystals (Wetterling et al., 2018). The energy demand of electroosmotic dewatering is decreased with a decreasing electric conductivity of the system (Wetterling et al., 2017a). Therefore, the economic and environmental aspect are dependent on how far the suspensions of cellulose nanocrystals are dialyzed in the production since the dialysis lowers the ionic strength of the system and thereby the electrical conductivity.

1.2 Aim

This project investigates how the electrical conductivity of suspensions of cellulose nanocrystals influence the electroosmotic dewatering behavior. The aim of the investigation is to determine at which conductivities electroosmotic dewatering may be used to decrease the energy demand compared to conventional drying methods.

The aim of the project is to increase the knowledge about how the electric conductivity influences the electroosmotic dewatering behavior of cellulose nanocrystals in terms of specific energy demand and dewatering rate. This knowledge will be important in the implementation on the technology of large scale industrial production and important in the design of cleaning of cellulose nanocrystals before use of electroosmotic dewatering.

1.3 Delimitations

- Cellulose nanocrystals will be produced on site through acid hydrolysis. However, optimization of the hydrolysis reaction and recovery of excess acid will not be considered in this study.
- Electroosmotic dewatering of cellulose nanocrystals will be studied, not cellulose nanofibrils.
- An existing equipment for electroosmotic dewatering will be used and equipment design and optimization is not considered in this study.

2 Theory

This chapter aims to provide necessary background information for the study. Section 2.1 focuses on cellulose and nanocelluloses and section 2.2 focuses on dewatering through filtration and electro-assisted filtration.

2.1 Cellulose

Cellulose is one of the most common polymers in nature and trees normally have a cellulose content of 40- 50% (Henriksson et al., 2009). It is built up by glucose units which are linked together by 1-4 glucosidic linkage of β-D-glucose, the structure is described in Figure 1. The polymers can be built up by as many as 20 000 units of glucose, how many units varies with the source of the cellulose (Henriksson and Lennholm, 2009).

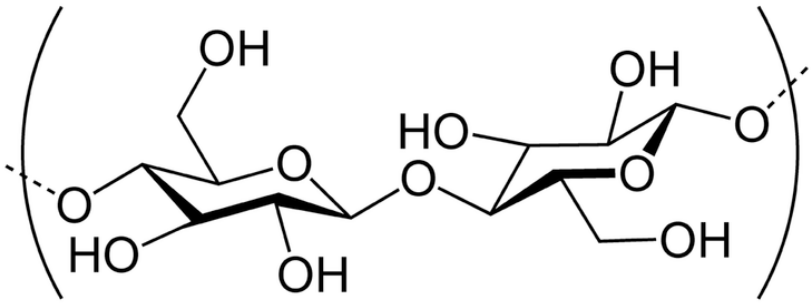

Figure 1. Molecular structure of cellulose.

2.1.1 Nanocelluloses

When a cellulose entity have at least one dimension in nanometer range it can be referred to as a nanocellulose. Cellulose nanocrystals and cellulose nanofibrils are two different categories of nanocelluloses. They are in some extent similar to each other as they have similar qualities such as high tensile strength and high specific surface area. But they have some noticeable differences. Cellulose nanocrystals have a high crystallinity while in cellulose nanofibrils amorphous parts of the cellulose remains (Börjesson and Westman, 2015).

2.1.2 Cellulose nanocrystals

The production of cellulose nanocrystals often starts with alkali treatment as pretreatment of microcrystalline cellulose. This is to remove contaminations such as hemicelluloses and pectins and to obtain a cellulosic material with high purity. After the pretreatment the main process is carried out which consist of acid hydrolysis. The acid hydrolysis results in single crystallites are released through breaking of glycosidic bonds in the amorphous parts through

addition of either sulfuric acid or hydrochloric acid (Dufresne, 2012). After the acid hydrolysis the cellulose nanocrystals have a rod-like shape (Abitbol et al., 2016) and normally have a width of 2-30 nm and a length of several hundred nanometers (Börjesson and Westman, 2015). The suspensions containing cellulose nanocrystals are post-treated to remove excess acid after the acid hydrolysis. This can be done either by dialysis or by diluting the suspensions in water and centrifuge it and then remove the water phase (Dufresne, 2012).

Cellulose nanocrystals are of interest for production of materials because of favorable properties such as high tensile strength, large surface area and optical properties (Peng et al., 2011). The crystals are also relatively easy to modify thanks to their large surface area and their functional groups. The functional groups consist of hydroxyl units, ester units and ether units and some common ways to modify the cellulose are through oxidation, etherification and esterification. For example cellulose nanocrystals can be made either hydrophilic or hydrophobic depending on what suits the product. One example is the use of hydrophobic surfaces as packaging materials. Cellulose nanocrystals can also be used as a filler material in thermoplastics or packaging material. The high tensile strength then provides bearing ability for the product (Abitbol et al., 2016).

2.1.3 Cellulose nanofibrils

Cellulose nanofibrils is often produced through mechanical treatment. This process breaks the bonds between the cellulose polymers but keeps the polymers themselves intact. This give the cellulose nanofibrils the same diameter as the cellulose nanocrystals, 2-30 nm, but the fibrils maintain their widely ranging length from approximately 100 nm to several micrometers. The long length of the fibers compared to their thickness makes the cellulose nanofibrils useful for composite materials, as they have the ability to greatly reinforce a polymer matrix (Börjesson and Westman, 2015).

2.2 Filtration

2.2.1 Dead end filtration

Filtration is a mechanical dewatering operation where the liquid in a suspension can pass through a filter medium but solid particles are retained. This leads to a buildup of a filter cake. The liquid thus have to move through both the filter medium and the filter cake. The permeability (K) of the filter cake can be determined with the help of Darcy's law and is shown below in equation 1: (Darcy, 1856)

$$K = \frac{Q\mu X}{A\Delta P} \qquad (1)$$

where A is the filter area, ΔP the pressure drop of the fluid over the filter cake, Q the flowrate of the fluid, μ the viscosity and X the thickness of the filter cake. The permeability is in turn used to calculate the specific filter cake resistance, equation 2:

$$\alpha = \frac{1}{K\rho_s\phi} \quad (2)$$

where α is the specific filter cake resistance, ρ_s the density of the solid material and ϕ the packing density of solid material (solidosity) in the filter cake.

The filtration behavior for incompressible filter cakes can be described by the filtration equation showed in equation 3:

$$\frac{dt}{dV} = \frac{\mu(\alpha cV + AR_m)}{\Delta P A^2} \quad (3)$$

Where c is the amount of solids per unit of filtrate, R_m the flow resistance of the filter medium and V the filtrate volume (Ruth, 1935).

Decreased filtration rate caused by the filter cake can partly be counteracted through increasing the applied pressure over the filter cake or vacuum pressure below the filter medium. When looking at equation 3 it can be seen that this can improve the filtrate flow rate. However, most materials are compressible since the particles deform, rearrange and break as a result off applied pressure (Shirato et al., 1969), which means that the solidosity of the filter cake increases with increased pressure. The increased solidosity affects the permeability of the filter in a way that can often be described by the Kozeny-Carman equation, equation 4:

$$K = \frac{(1-\phi)^3}{kS_p^2\phi^2} \quad (4)$$

where k is the Kozeny-Carman constant and S_p is the specific surface area of the material (Kozeny, 1927, Carman, 1937). Increased solidosity leads to decreased permeability, and if increased pressure increases the solidosity, the effect on the flow rate by increasing the applied pressure may be limited. The permeability is low due to the large specific surface area of the cellulose nanocrystals leading to further limitations on dewatering rate through increasing the applied pressure. In this case assisted filtration can be a good option.

2.2.2 Electro-assisted filtration

Filtration of materials that form compressible filter cakes (such as cellulose nanocrystals) can be improved by the use of assisted filtration. A number of different techniques for assisted filtration exist. A few examples are *thermal mechanical dewatering* where increased

temperature is used to lower the viscosity of the fluid, *magnetic mechanical dewatering* where magnetic forces are used to separate minerals, *acoustic mechanical dewatering* where ultrasonic vibrations are used to separate a solid/liquid system and *electro-assisted filtration* where the particles charge are used to increase the solid/liquid separation by applying an electric field (Mahmoud et al., 2010).

Since the particles in cellulose nanocrystals and micro fibrillated cellulose are negatively charged electro-assisted filtration have shown potential for increasing the dewatering rate during filtration (Wetterling, 2017). The electric field gives electrophoresis of charged particles inside the electric field, as described in Figure 2, which can reduce the buildup of a filter cake. The electric field also causes an extra driving force for separation through electroosmosis. However, the electric field have a couple of side effects; ohmic heating causing the temperature to rise in the filter cell and electrolysis reactions occur at the electrodes (Mahmoud et al., 2010). These concepts are further discussed in the following sections.

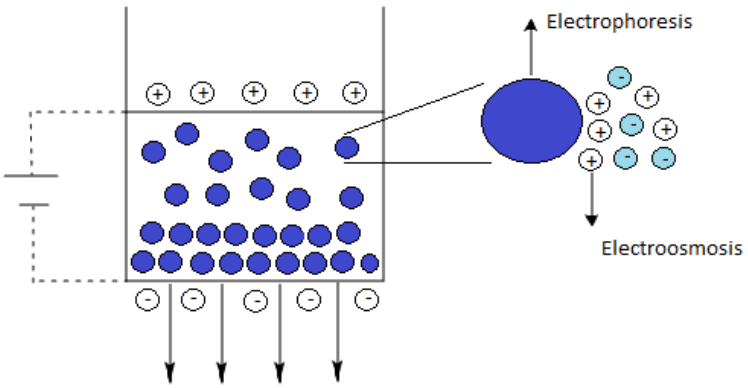

Figure 2. Basic principle of electro-assisted filtration.

2.2.2.1 Electrophoresis

Charged particles in an electric field are affected by a force in the direction of the oppositely charged electrode. This causes a movement of the charged particles towards the oppositely charged electrode and the movement continues until the particle is stopped by either a filter, filter cake or until the fluids resistance becomes too high. The filter medium is placed over the systems cathode and therefore negatively charged particles are repelled from the medium. The velocity of the particles can be described by the Helmholtz-Smoluchowski equation for electrophoretic velocity (v_e) given in equation 5. Equation 5 is valid if the particles radius is larger than the electrical double layer (Debye length).

$$v_e = \frac{D\mathcal{E}_0\zeta}{\mu}\mathrm{E} \quad (5)$$

μ is the viscosity of the fluid, $\mathcal{E}_0$ the vacuum permeability and D the dielectric constant of the liquid phase, ζ the zeta potential (potential of the electrical double layer) and E the strength of the electric field.

The Debye length is formed around charged particles in a suspension as the particles surface charges attracts oppositely charged ions in the suspension. It is a measure of the electrical double layers length around a particle and its length can be calculated with equation 6:

$$\kappa^{-1} = \sqrt{\frac{\mathcal{E}_{rs}\mathcal{E}_0 k_b T}{2N_A e^2 I_{is}}} \quad (6)$$

where k_b is the Boltzmann constant, N_A the Avogadro constant, e the elementary charge, T the temperature and I_{is} the ionic strength of the system.

For particles where the radius is of the same order of magnitude as the Debye length (which the particles often are if the particles radius is within nanoscale) the effect of the electrical double layer on the particle have a wider range than the particles radius. Then the Debye-Hückel equation, which is shown in equation 7, can be used to describe the velocity of the particles (Hiemenz and Rajagopalan, 1997).

$$v_e = \frac{2\mathcal{E}_{rs}\mathcal{E}_0\zeta}{3\mu}\mathrm{E} \quad (7)$$

2.2.2.2 Electroosmosis

Electroosmosis is an effect of acceleration of ionic components in the electrical double layer surrounding charged particles. This acceleration gives an acceleration of the bulk fluid between particles as a result of viscous forces. The resulting movement of the liquid bulk gives an electroosmotic separation of solid from liquid. The Helmholtz-Smoluchowski equation can be used to describe the electroosmotic flow rate and is given by equation 8:

$$Q_{eo} = -\frac{D\zeta\mathcal{E}_0}{\mu} E A_c \quad (8)$$

where Q_{eo} is the electroosmotic flow rate and A_c the cross-sectional area of the capillary (Lyklema, 1995).

For suspensions of nanoparticles with a low ionic strength, it can be assumed that the solid particles are in the same order as the Debye length. The systems electrical conductivity may

therefore be strongly affected by the solid particles surface conduction. This effect can be accounted for by modifying equation 8, this results in equation 9:

$$Q_{eo} = -\frac{D\zeta\varepsilon_0}{\mu} A_c E(1 - G(\kappa a)) \quad (9)$$

where a is the radius of the capillary and k the Debye length. G(κa) is in turn given by equation 10:

$$G(\kappa a) = \frac{2I_1(\kappa a)}{\kappa a I_0(\kappa a)} \quad (10)$$

in equation 10 I_0 and I_1 are given by the modified Bessel functions. However equation 9 should only be used for small values on κa since if the value is large the surface conductivity can be neglected due to the radius being larger than the Debye length and equation 8 can be used (Delgado et al., 2007).

2.2.2.3 Electrolysis reactions

Electrolysis reactions take place at the electrodes and are affected by the ions in the suspensions. The reactions are different depending on which electrode they occur at and equation 11 and 12 describe the reactions at the anode while equation 13 and 14 describe the cathode.

$$2H_2O \rightarrow O_{2,(g)} + 4H^+ + 4e^- \qquad E_0 = 1.23V \quad (11)$$

$$M \rightarrow M^{n+} + ne^- \quad (12)$$

$$2H_2O + 2e^- \rightarrow 2OH^- + H_2 \qquad E_0 = -0.83V \quad (13)$$

$$M^{n+} + ne^- \rightarrow M \quad (14)$$

M is the material the electrodes are composed of and E_0 is the standard electrode potential for the reactions at 298 K. As can be seen in the equations the electrode material effect the reactions. This may lead to corrosion of the anode. The material for the anodes are therefore chosen as materials more resistant to corrosion for example titanium meshes coated with metal oxides (Mahmoud et al., 2010). The reactions also cause acidic conditions at the anode and alkaline conditions at the cathode. A pH profile is therefore established between the electrodes. How much the conditions change at the electrodes varies with the amount of electrolysis products (n_p) that are produced when the electric field is active which is given by equation 15:

$$n_p = \frac{\lambda I t}{nF} \quad (15)$$

F is the Faraday constant, n amount of electrons, λ the stoichiometric coefficient of the electrolysis reactions, I the current and t is time (Larue and Vorobiev, 2004).

The current is dependent on the strength of the electric field. Which in turn is proportional towards the electrical conductivity (k) of ions in the suspension as the resistance decreases when the conductivity increases according to equation 16:

$$k = \frac{l}{A*R} \quad (16)$$

where l is the length between the electrodes and A the cross sectional area (Atkins and Jones, 2010). Since H^+ ions have high electrical conductivity (Adamson, 1979) the resistance in the suspension will decrease gradually as long as the electric field is active since the electrolysis reactions produce H^+ ions which then increases the suspensions conductivity.

2.2.2.4 Ohmic heating

Ohmic heating arise when a current is set through a system and leads to an increase in temperature. The temperature rises due to the electrical resistance and equation 17 can be used to describe the ohmic heating (Q):

$$Q = I^2 R \quad (17)$$

where R is the resistance and I the applied current (Curvers et al., 2007).

The temperature increase decreases the viscosity of the fluid. However, if the temperature becomes too high it might damage the particles (Loginov et al., 2013). The current becomes higher for a system with higher conductivity if the voltage is kept constant as the resistance decreases according to equation 16. This might result in very high ohmic heating since the heating is proportional to the square of the current.

3 Experimental

This section describes how the experiments in the project were carried out. Section 3.1 describes how the cellulose nanocrystals were made, section 3.2 describes how the crystals were characterized and section 3.3 describes how the electroosmotic dewatering experiments were performed.

3.1 Production of cellulose nanocrystals

3.1.1 Acid hydrolysis

The cellulose nanocrystals were produced through acid hydrolysis using a procedure described in previous publications (Hasani et al., 2008, Sahlin et al., 2018). Four liters of 64 weight % sulfuric acid was preheated to 45 ^{o}C and 500 g of microcrystalline cellulose (PH101, Avicel) was added. The hydrolysis was performed for 2 hours at constant temperature in a well-mixed vessel. The reaction was quenched by addition of twelve liter of deionized water at room temperature.

3.1.2 Dialysis

After the hydrolysis excess acid was removed through dialysis. Dialysis was performed by adding approximately 250 ml suspension to dialysis tubing membrane (D9402, Sigma). The membrane tubes were completely covered with deionized water and the deionized water was changed frequently. During the dialysis the membranes swelled to a volume of approximately 400 ml. The dialysis was stopped at different times to get different electrical conductivity levels for the suspensions, see Table 1.

Table 1. pH and conductivity for suspension of cellulose nanocrystals after different degrees of dialysis.

Suspension number	Conductivity [mS/cm]	pH
Susp 1	30.9	0.95
Susp 2	22.1	1.26
Susp 3	12.4	1.59
Susp 4	8.50	1.63
Susp 5	4.40	1.98
Susp 6	2.50	2.23
Susp 7	1.20	2.40
Susp 8	0.67	2.58
Susp 9	0.34	2.80

After the dialysis the suspensions were either pH adjusted to pH 5 or not changed from their original conditions. This was done so that the suspensions could be tested at the same pH

values and at their original conditions. The pH adjustment was done with 1M NaOH and after the adjustment the conductivity was measured.

3.1.3 Sonication

After the dialysis the cellulose particles were dispersed through ultrasonic treatment. The suspensions were sonicated to reach a dispersed state with a Sonics Vibracell 500 W equipped with a standard probe with tip diameter of 13 mm operating at 40% of maximum amplitude for 6 minutes. The treatment was repeated 7-9 times to reach a colloidal dispersion. The suspensions below pH 2 were excluded from the experiments at their original conditions since the sonication equipment was limited to use above pH 2 which meant that the dispersed state could not be achieved. However, the suspension with pH 1.63 were adjusted to pH 2 to be tested with the suspensions at the original conditions. After the sonication the pH, conductivity and solid content of the suspensions were measured.

3.2 Characterization

Cellulose nanocrystals produced according to the procedure described in section 3.1 have been characterized in previous publications (Börjesson et al., 2018). In this study a number of characterizations were carried out including Atomic force microscopy (AFM), IR-spectroscopy, conductivity titration, ζ potential and solid content.

The AFM analysis was carried out to give the dimensions of the nanocrystals. The analysis was performed with a Digital Instrument nanoscope III equipped with a type G scanner (Digital Instruments INC, Santa Barbara, Ca). The cellulose nanocrystals were diluted to a concentration of 10 ppm solid content before the analysis in order to see the single cellulose nanocrystals.

The IR-spectroscopy was carried out to confirm that cellulose nanocrystals had been produced. The analysis was carried out in a Perkin Elmer Frontier FTIR Spectrometer (Waltham, MA) equipped with attenuated total reflectance device and the crystals were analyzed between 4000 and 400 cm^{-1} and a resolution of 4 cm^{-1} was used. The cellulose nanocrystals were completely dried before running.

Conductivity titration was performed to measure the sulfur content of the cellulose nanocrystals. Samples were diluted to 1.2 weight % and were then ion exchanged with Dowex Marathon MR-3. The samples were then further diluted to 0.036 weight % by mixing it with 1 mM NaCl. 200 µl of 2 mM NaOH was then added with one minute intervals until the conductivity had increased enough to plot a linear trend line.

The ζ potential was measured in a Zetasizer Nano ZS (Malvern Instruments, Malvern, UK). The cellulose nanocrystals were diluted to 0.05 weight % and ion exchanged with Dowex Marathon MR-3.

The solid content of the suspensions of cellulose nanocrystals was measured before and after the electroosmotic dewatering. The measurement was carried out through drying where all liquids were evaporated and the sample was weighted before and after the drying.

3.3 Electroosmotic dewatering

Electroosmotic dewatering experiments were performed in a filter cell with two platina electrodes. The distance between the electrodes is 2.5 cm and the dimensions of the filter cell is given in Figure 3. The cathode had a mesh of 1 cm separation and the anode tight mesh (Unimesh 300). The diameter is decreased from 6 cm to 5 cm for the section between the electrodes because of a support track for the electrodes. The filter medium used for the experiments had a pore size of 0.1 µm (Supor®-100 Membrane Filter, Pall Corporation) and was placed above the cathode electrode. The experiments were performed at either a constant applied current of 0.3 A or constant applied voltage of 5 V/cm. The filtrate weight is measured on a scale below the filter cell, the temperature is measured at two places between the electrodes and the cell is open to the atmosphere.

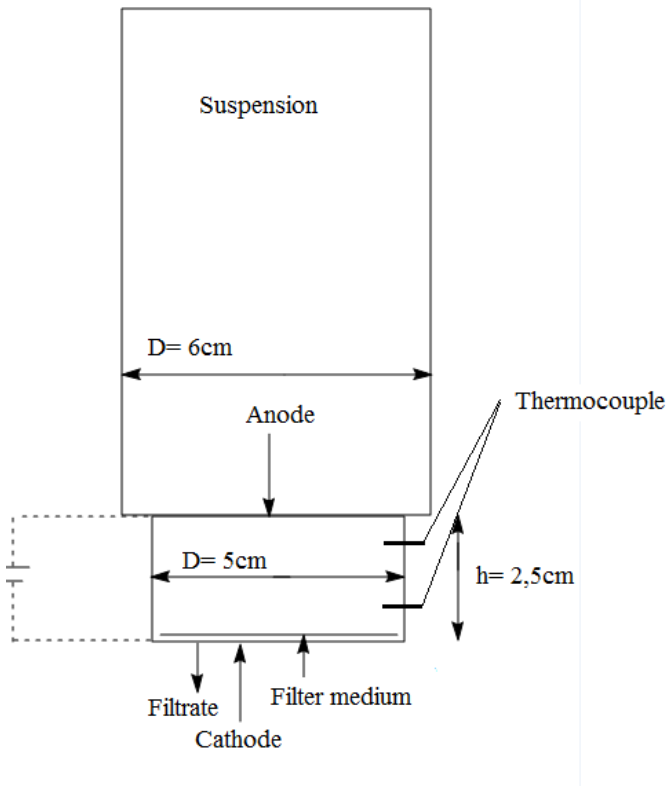

Figure 3. Drawing of filter cell used during the dewatering experiments.

4 Results and Discussion

In this chapter the experimental results are presented and discussed. Section 4.1 focuses on the characterization of cellulose nanocrystals and the suspensions containing the cellulose nanocrystals and section 4.2 focuses on the electroosmotic dewatering of the cellulose nanocrystals.

4.1 Characterization

4.1.1 Cellulose nanocrystals

A picture of the cellulose nanocrystals from AFM analysis is shown in Figure 4. The cellulose nanocrystals are rod-shaped with a diameter ranging from 4 nm to 6 nm and a length ranging from 150 nm to 600 nm. The results were similar to previous publications producing cellulose nanocrystals with the same procedure (Börjesson et al., 2018, Moberg et al., 2017).

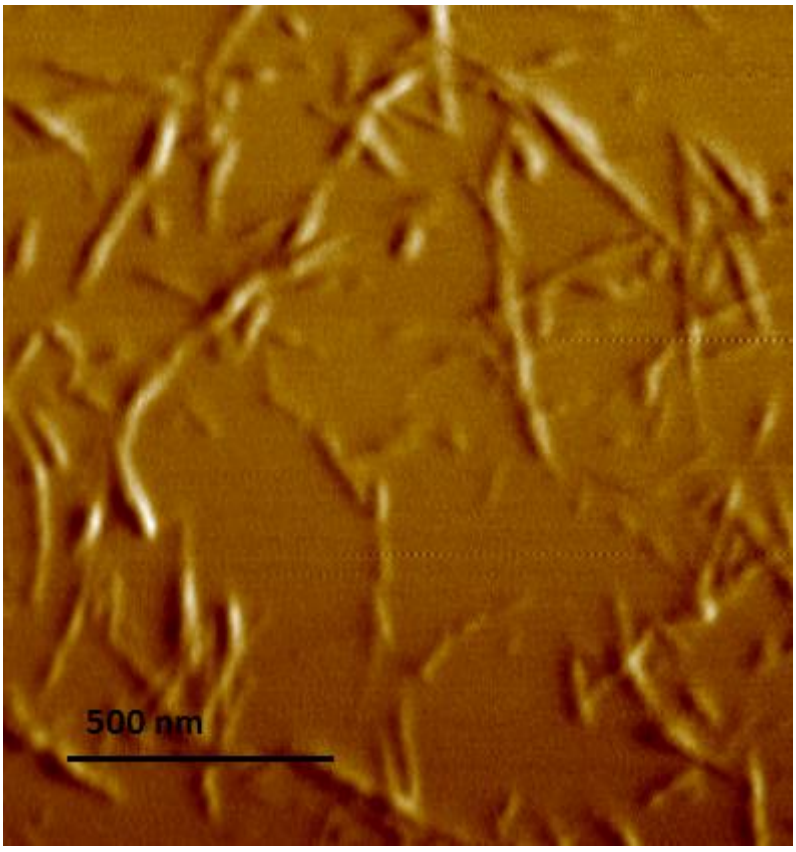

Figure 4. AFM picture of the cellulose nanocrystals used in this study.

Results from IR- spectroscopy of the produced cellulose nanocrystals are shown in Figure 5. The results are in agreement with previous publications confirming that cellulose nanocrystals have been produced and no other side reactions have taken place (Sahlin et al., 2018).

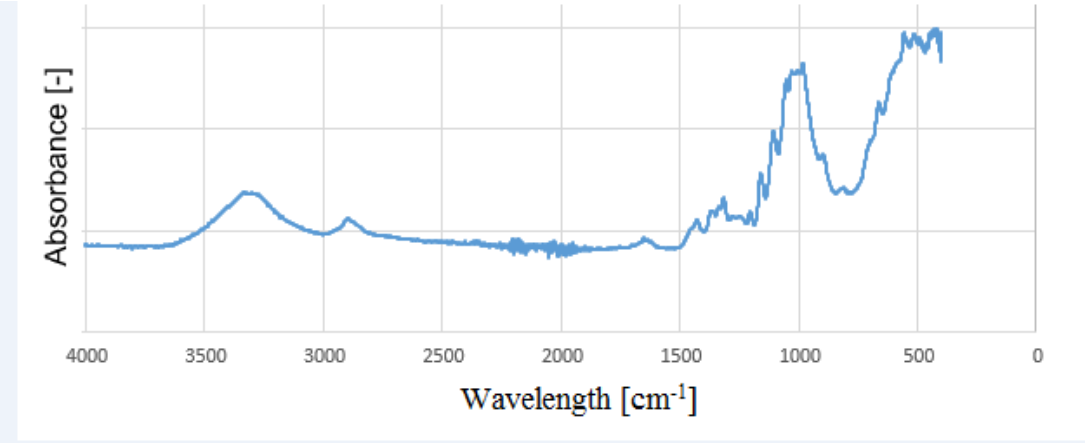

Figure 5. Absorbance in IR spectrum from 4000 cm^{-1} to 400 cm^{-1} for cellulose nanocrystals after dialysis.

The results from conductivity titration showed that the cellulose nanocrystals had a sulfur content of 1.05 weight %. The results from the analysis of the zeta potential showed that the cellulose nanocrystals had a zeta potential of -75 ± 7 mV. The cellulose nanocrystals were analyzed at different conductivity levels and no significant difference could be seen between them leading to that the dialysis does not affect the charge of the cellulose nanocrystals significantly with the procedure used in this study.

4.1.2 Suspension conditions

After the dialysis the cellulose nanocrystals were dispersed through ultrasonic treatment and the conductivity and pH of the suspension was measured, see Table 2. The pH of suspension 4 was adjusted to pH 2 before the ultrasonic treatment due to the limitations of the treatment probe. The sonication was found to result in an increasing conductivity, an effect that was more pronounced for systems with a low electrical conductivity. This behavior indicates that the surface conduction has a larger impact on the conductivity for suspensions with lower conductivities as mentioned in section 2.2.2.2.

Table 2. pH, conductivity and solid content for suspensions 4-9. Note that suspension 4 was adjusted to pH=2.

Suspension	pH	Conductivity [mS/cm]	pH Sonicated	Conductivity Sonicated [mS/cm]	Solid content [Weight %]
Susp 4	2.00	5.40	2.00	5.50	1.57
Susp 5	1.98	4.40	1.98	4.60	1.45
Susp 6	2.23	2.50	2.22	2.60	1.55
Susp 7	2.40	1.20	2.40	1.50	1.34
Susp 8	2.58	0.67	2.50	1.10	1.39
Susp 9	2.80	0.34	2.60	0.87	2.01

Experiments were also performed for suspensions were the pH was adjusted to pH 5 before the ultrasonic treatment. The suspension conditions after pH adjustment and sonication are shown in Table 3. The pH adjustment lowered the conductivity significantly compared with Table 1 since H^+ ions were removed, even if the ionic strength increased through the addition of the NaOH. The sonication showed the same trend as for the systems without pH adjustment as the electrical conductivity increased during sonication and the increase was larger for suspensions with lower conductivities. Suspensions 4-9 were successfully dispersed during the ultrasonic treatment. However, suspensions 1-3 did not become fully dispersed as the ionic strength was too high to successfully produce dispersed cellulose nanocrystals. For this reason suspensions 1-3 will not be analyzed in the electroosmotic dewatering section.

The solid content were even between the suspensions with somewhat decreasing trend for longer dialysis times due to swelling of the membrane tubes filled with suspension. The difference between the obtained suspensions could also be attributed to variations of the initial volume of suspension in the membrane tubes.

Table 3. pH, conductivity and solid content for suspensions after pH adjustment and sonication.

Suspension	pH adjusted	Conductivity pH adjusted [mS/cm]	pH sonicated	Conductivity sonicated [mS/cm]	Solid content [Weight %]
Susp 1	5.23	8.80	5.08	9.00	2.03
Susp 2	5.00	6.60	5.20	6.60	1.84
Susp 3	5.10	3.80	5.26	3.90	1.99
Susp 4	5.10	2.60	5.10	2.60	1.57
Susp 5	5.00	1.30	5.14	1.30	1.45
Susp 6	5.00	0.76	4.96	0.77	1.55
Susp 7	5.10	0.30	5.11	0.35	1.34
Susp 8	5.10	0.16	5.00	0.22	1.39
Susp 9	5.10	0.07	5.00	0.15	2.01

4.2 Electroosmotic dewatering

4.2.1 Influence of the electric field

4.2.1.1 Dewatering rate

Figure 6 shows how the solid content between the electrodes increases over time as water is removed. Constant applied current increases the solid content between the electrodes rapidly in the early parts of the dewatering experiments and later the dewatering rate decreases towards the end of the experiment. The constant applied voltage gave a dewatering rate that were more stable throughout the entire experiment.

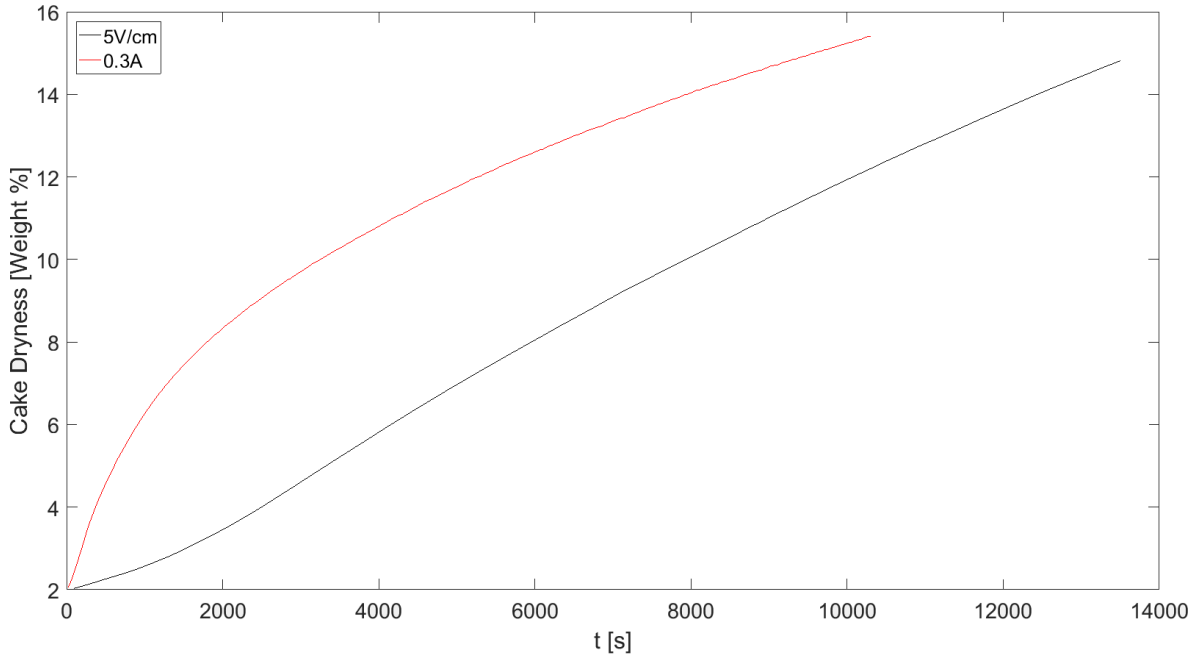

Figure 6. Cake dryness over time for electroosmotic dewatering of a suspension of cellulose nanocrystals at pH 5 and 0.15 mS/cm for either constant applied voltage or current.

To explain this behavior the applied voltage and dewatering rates during the experiments are studied. The applied voltage is shown in Figure 7 and it can be seen that the voltage for the experiment with a constant applied current is initially high but quickly decreases and towards the end the voltage is equal between both experiments. The decreasing voltage in the experiment with constant applied current comes as a result of decreased resistance due to a combination of electrolysis reactions and an increasing solid content between the electrodes. The increased amount of H^+ ions from the electrolysis reactions also reduces the pH and thereby hinders the electroosmotic dewatering as the negative charges on cellulose nanocrystals are neutralized by H^+ ions.

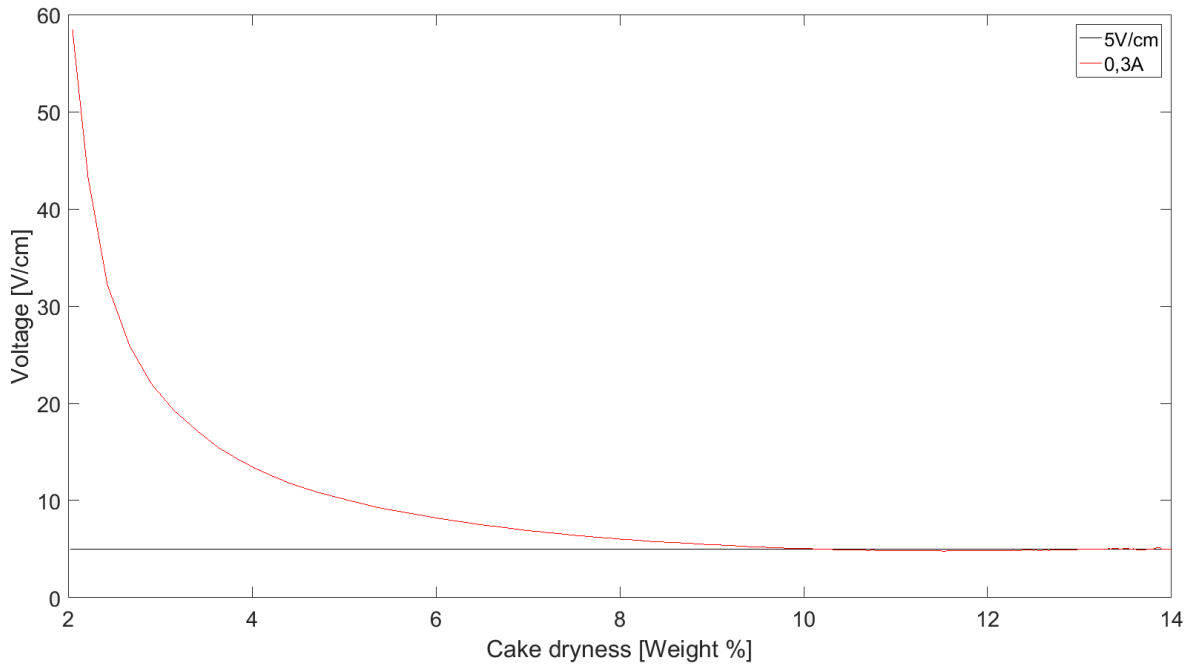

Figure 7. Applied voltage during the electroosmotic dewatering of a suspension at pH 5 and 0.15 mS/cm for constant applied voltage and current.

The electroosmotic dewatering rate is shown in Figure 8 for experiments performed at either a constant applied current or voltage. The dewatering increases quickly in the beginning of the experiments, this is likely an effect of a small startup time in the equipment before obtained filtrate is registered on the scale below the filtration equipment. When comparing the constant applied current to the constant applied voltage a much more stable dewatering rate is obtained for the constant applied voltage and the dewatering rate decreases faster during the experiments for the constant applied current. This effect indicates that voltage have a more dominant effect on the dewatering rate than the current. This belief gains strength since when the voltage reaches the same level for the experiments so does the dewatering rate and higher voltage gives a higher dewatering rate. This effect is in agreement with the Helmholtz-Smoluchowski equation, see equation 8.

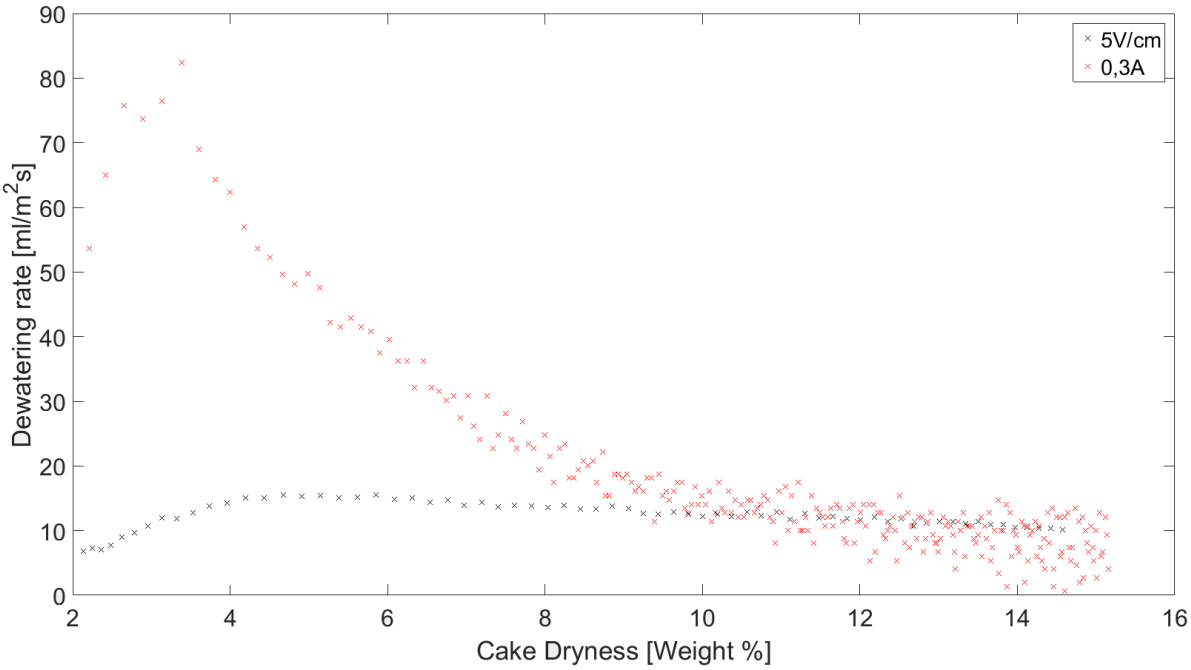

Figure 8. Dewatering rate for suspensions of cellulose nanocrystals at pH 5 and 0.15 mS/cm constant applied voltage and current.

4.2.1.2 Energy demand

The specific energy demand for the electroosmotic dewatering is shown in Figure 9. The experiments at constant applied current had higher energy demand during the early stages of the dewatering operation. This is a result of the lower voltage in the constant applied voltage experiment leading to lower current which resulted in less ohmic heating and thereby a lower temperature increase during constant applied voltage experiment as can be seen in Figure 10. It can be seen that the difference in energy demand grows smaller towards the end of the experiment. This a result of the voltage and resistance becoming equal between the experiments leading to equal current as well. The equal current makes the ohmic heating equal between the experiments and thereby the same energy losses occur. This is in agreement with previous publications (Wetterling et al., 2017b) as increased voltage leads to more ohmic heating through a higher current.

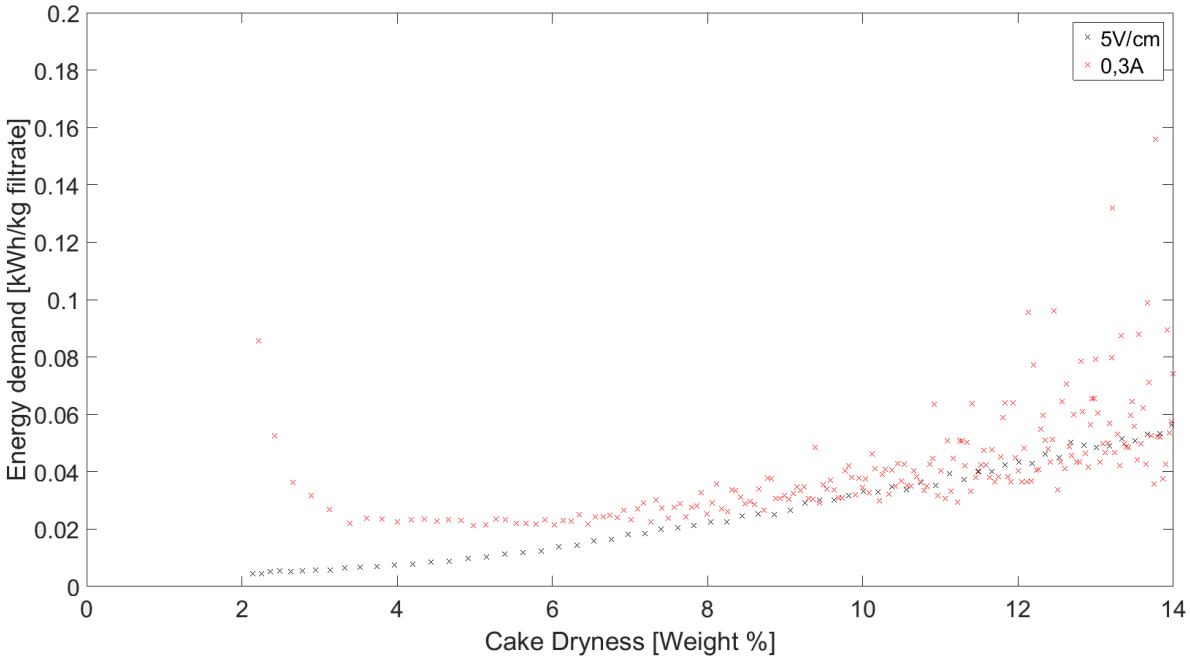

Figure 9. Energy demand for a suspension of cellulose nanocrystals at pH 5 and 0.15 mS/cm.

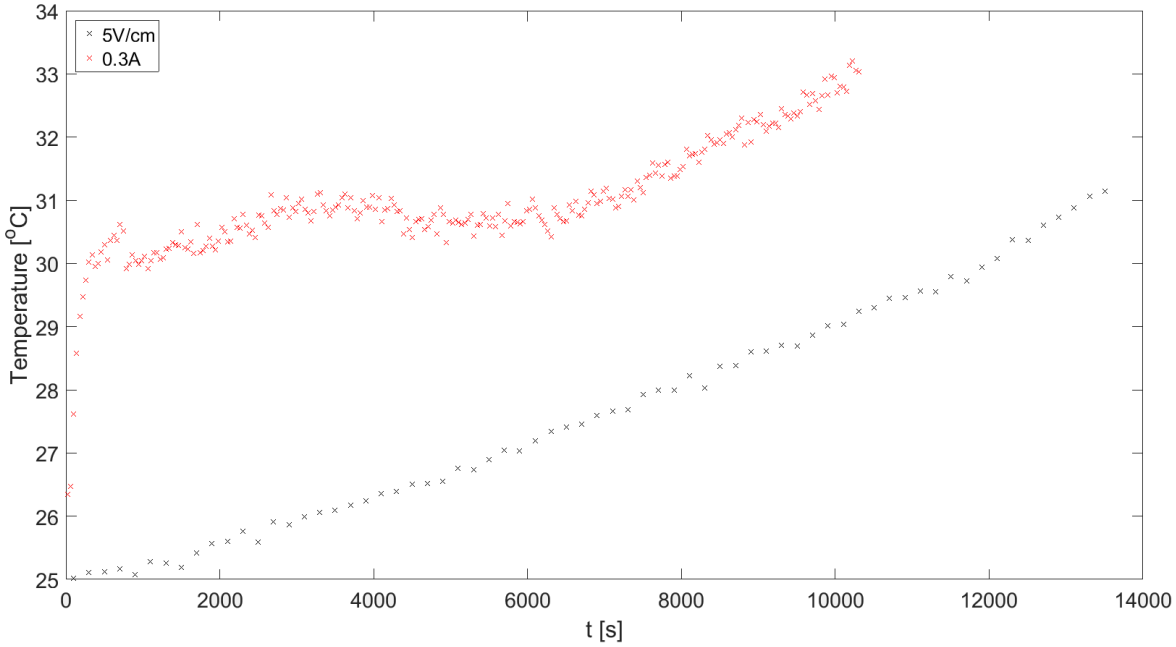

Figure 10. Temperature for a suspension of cellulose nanocrystals at pH 5 and 0.15 mS/cm.

4.2.2 Influence of suspension pH

4.2.2.1 Dewatering rate

The pH in a suspension influences the electrical conductivity of the system and may affect the charge of the particle surface. The suspension pH may therefore have a large influence on the electroosmotic dewatering behavior. Suspensions at the same level of dialysis was therefore compared with and without pH adjustment.

Figure 11 shows a comparison of the electrical resistance between a suspension at the highest degree of dialysis with and without adjustment of the pH. It can be seen that the suspension with pH 5 was affected more in the early parts of the experiment than the suspension with pH 2.6. This is a result of the electrolysis reactions changing the suspension conditions as the conductivity is increased and the pH is lowered. Since the suspension with pH 2.6 had higher conductivity and lower pH the effect became lower as can be seen in Figure 11 since the electrical resistance decreased to a higher extent for the suspension at pH 5.

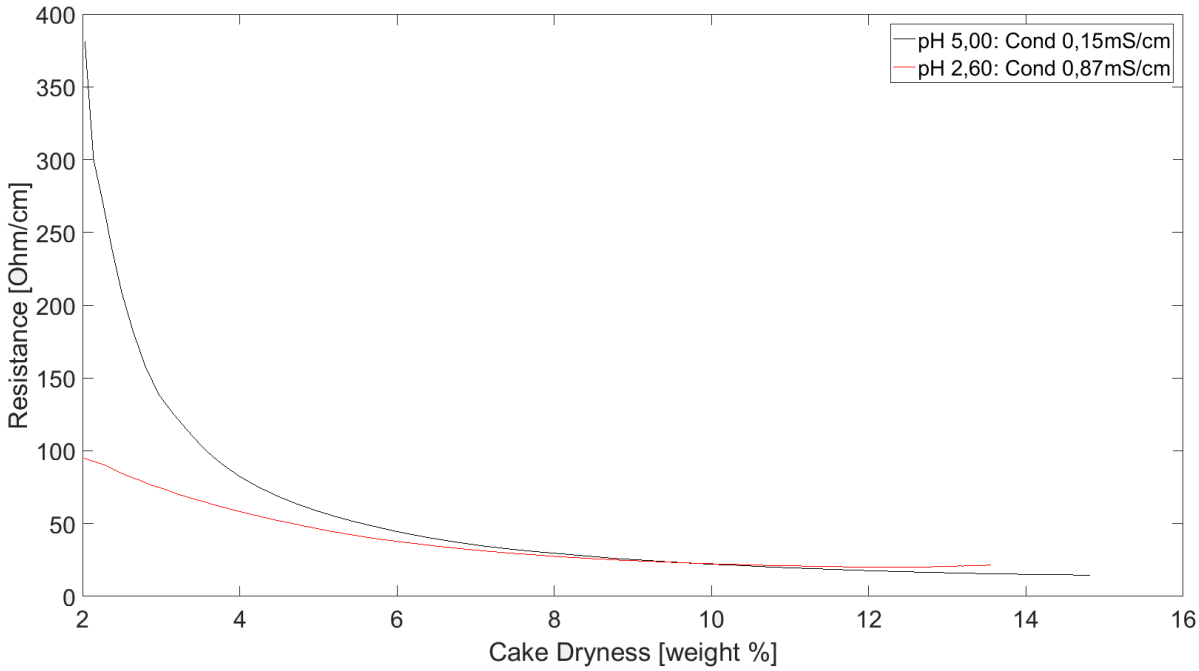

Figure 11. Resistance during electroosmotic dewatering with an applied voltage of 5 V/cm for suspensions either with or without adjustment of the suspension pH.

Figure 12 shows the corresponding dewatering rate for the experiments given in Figure 11. The startup time was shorter for the suspension without pH adjustment, however, suspensions at pH 5 received a somewhat higher maximum dewatering rate. Experiments performed at pH 5 were found to have somewhat higher dewatering rate throughout the later parts of the experiment. This behavior indicates that lower pH of the suspension leads to negative charges on the cellulose nanocrystals have been neutralized.

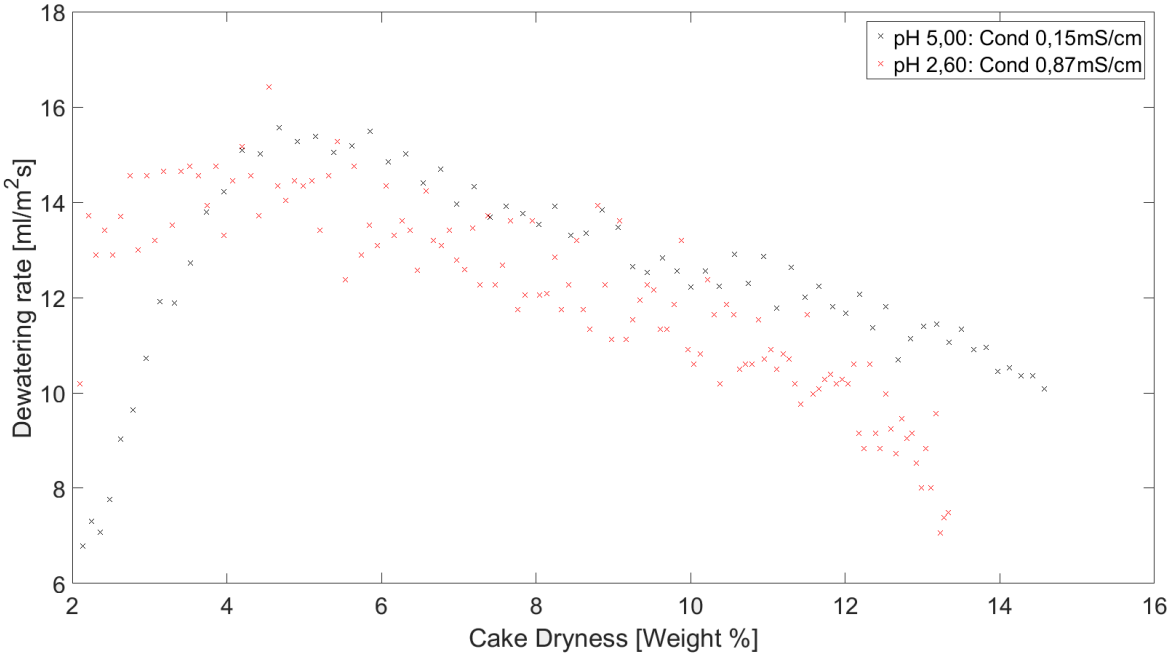

Figure 12. Dewatering rate during electroosmotic dewatering with an applied voltage of 5 V/cm for suspensions either with or without adjustment of the suspension pH.

4.2.2.2 Specific energy demand

In Figure 13 the energy demand for the experiments can be seen. It shows that both have the same magnitude of energy demand although the suspension at pH 5 have a somewhat lower energy demand than the suspension at pH 2.6. The suspensions at pH 5 had lower energy demand since its conductivity was lower. Lower conductivity leads to lower current and thereby less ohmic heating.

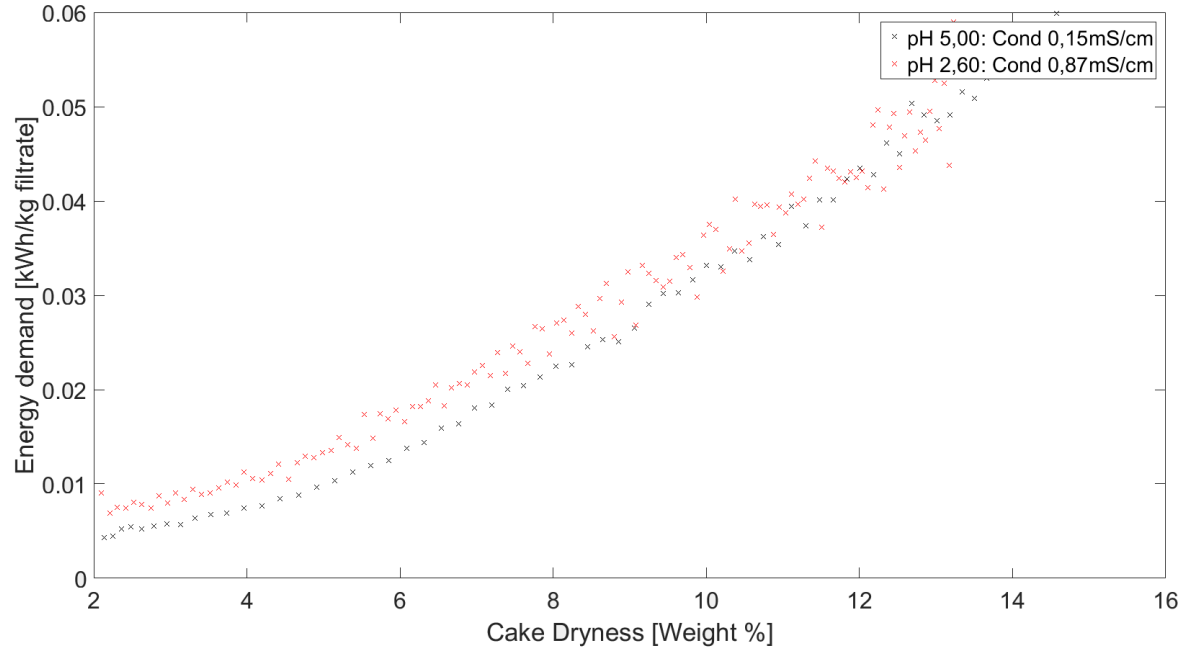

Figure 13. Energy demand during electroosmotic dewatering with an applied voltage of 5 V/cm for suspensions either with or without adjustment of the suspension pH.

4.2.3 Influence of suspension conductivity

4.2.3.1 Constant applied current

4.2.3.1.1 Dewatering rate

Figure 14 shows the applied voltage for experiments with constant applied current. When analyzing how the different conductivity levels affects the electroosmotic dewatering behavior it can be seen that the initial voltage becomes higher for lower conductivities. This makes the dialysis of great importance for the initial part of the constant applied current experiments since increased voltage increases the dewatering rate.

The voltage decrease during the dewatering experiments as a result of electrolysis reactions which reduces the resistance and towards the end of the experiments it have the same value for all suspensions except for the suspension with an initial conductivity of 1.3 mS/cm. The reason why the suspension with 1.3 mS/cm shows a different result in Figure 14 is that pyrolysis reactions occurred between the electrodes and formed a black layer on the cellulose nanocrystals at the anode. The pyrolysis reactions both damaged the cellulose nanocrystals and increased the resistance significantly (Wetterling et al., 2018).

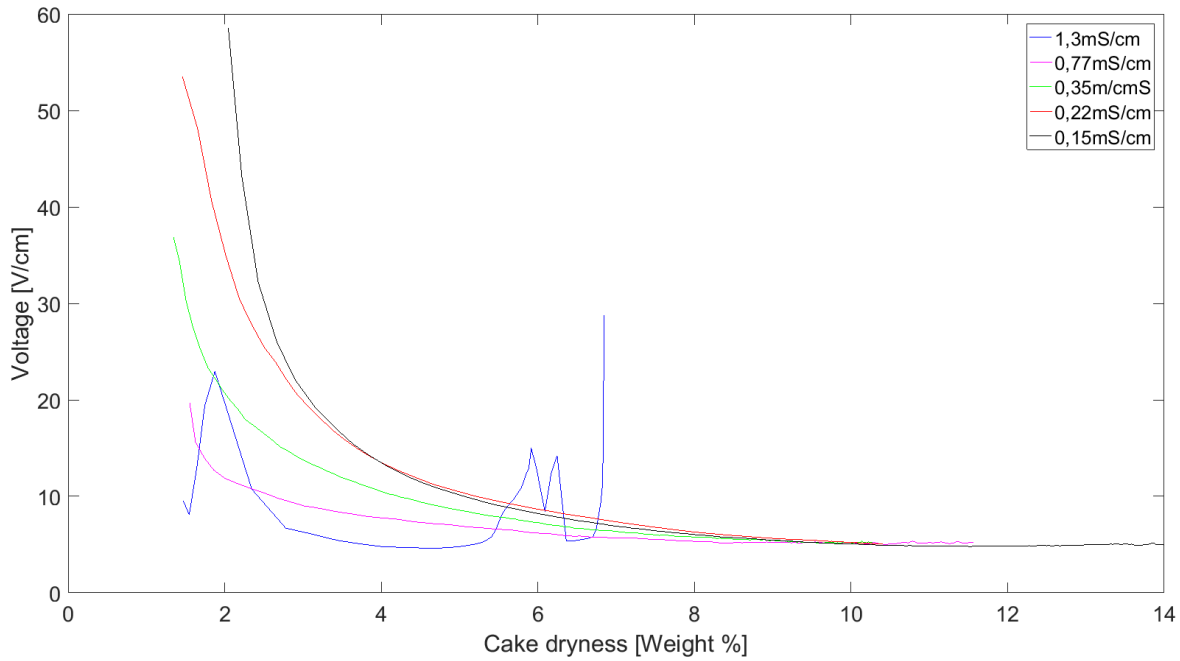

Figure 14. Voltage during dewatering experiments with a constant applied current of 0.3A for suspensions of cellulose nanocrystals at pH 5 and various electrical conductivities.

Figure 15 shows that the dewatering rate drops significantly in the beginning of the constant applied current experiments and then stabilizes on the same value for all suspensions were no pyrolysis reactions occurred. This comes as a result of the electrolysis reactions lowering the

pH and increasing the electrical conductivity to the approximately same level for all suspensions. This behavior is the same as shown in Figure 14.

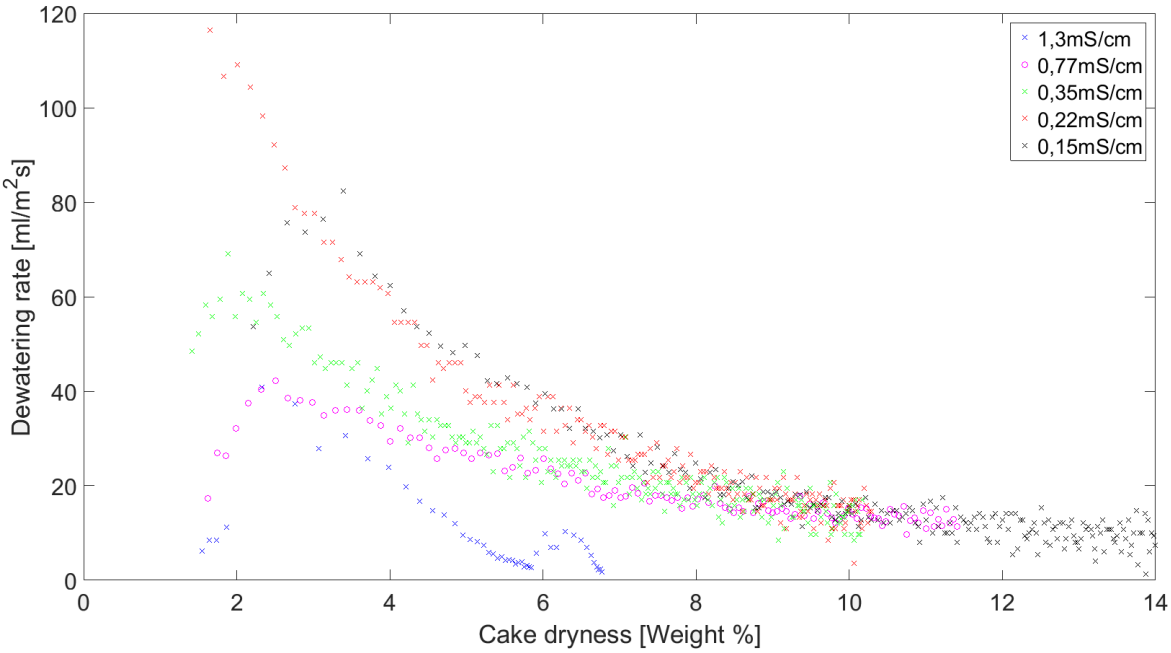

Figure 15. Dewatering rate during dewatering experiments with constant applied current 0.3A and pH 5 for various electrical conductivities.

4.2.3.1.2 Energy demand

The energy demand for all experiments with constant applied current of 0.3 A where no pyrolysis occurred are shown in Figure 16. The energy demand begin at higher levels and then decreases due to the low registered flow rate in the beginning of the experiment. The energy demand increases in the end of the experiments due to an increasing conductivity leading increased ohmic heating. The energy demand of the suspension with 1.3 mS/cm were excluded since the pyrolysis reactions increased the energy demand tenfold compared to the other suspensions.

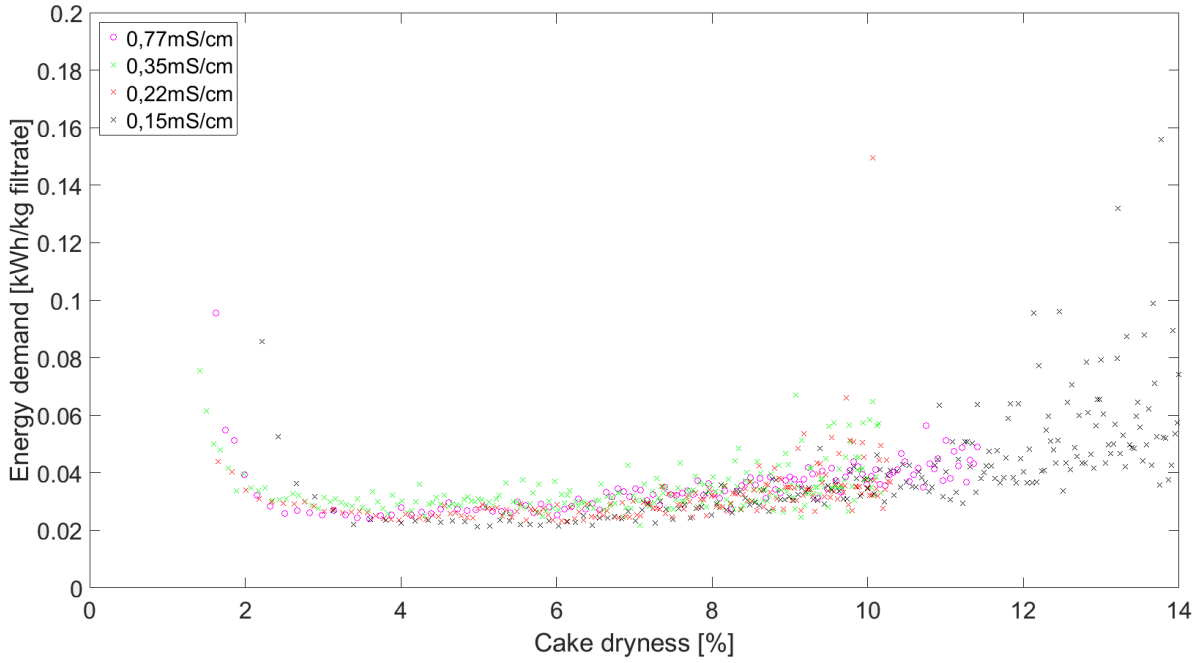

Figure 16. Energy demand during dewatering experiment with constant applied current for suspensions at pH 5.

4.2.3.2 Constant applied voltage

4.2.3.2.1 Dewatering rate

The dewatering rate for suspensions at different conductivity levels without pH adjustment at constant applied voltage are given in Figure 17. For the suspensions with 5.5 mS/cm and 4.6 mS/cm pyrolysis reactions occurred in the filter cake at the anode which resulted in a drastic decrease in dewatering rate. For the suspensions where successful dewatering was carried out the most dialyzed suspension with an initial conductivity of 0.87 mS/cm showed the highest dewatering rate throughout the experiment as the dewatering rate for the other suspensions decreased faster. The suspensions with conductivities between 1.1 mS/cm and 2.6 mS/cm showed almost identical dewatering rates making the dialysis of very little importance between these stages in terms of dewatering rate.

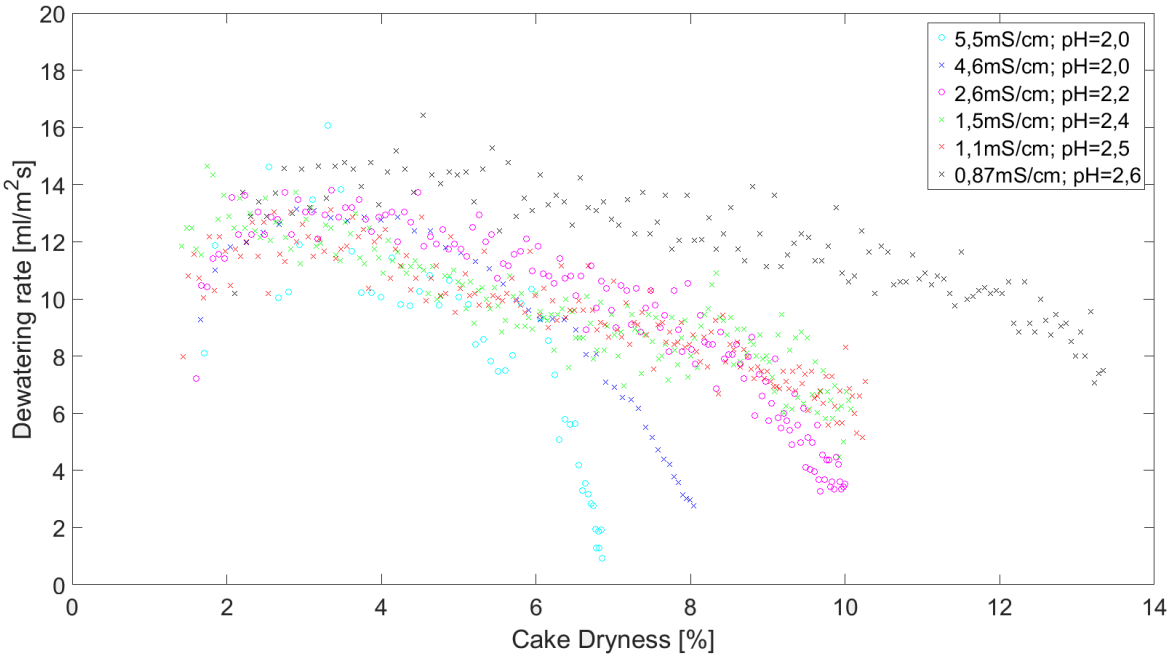

Figure 17. Dewatering rate during experiments with constant applied voltage of 5 V/cm for suspensions of cellulose nanocrystals with various electrical conductivities and pH values.

Figure 18 shows the dewatering rate for suspensions at pH 5 with constant applied voltage. It can be seen that the suspensions with 0.77 mS/cm or lower showed better dewatering behavior than the ones with higher conductivities. The reason for why the suspension with 2.6 mS/cm had lower dewatering rate than the lower conductivities was because that pyrolysis reactions took place. For the suspension with 1.3 mS/cm almost no dewatering happened at all. This was because that the electrical resistance increased significantly and stopped the dewatering completely.

Suspensions that were removed from the dialysis with electrical conductivities of 8.5 mS/cm and 4.4 mS/cm could not be dewatered with electroosmosis at an electric field of 5 V/cm, neither with nor without pH adjustment. This behavior indicates that pH adjustment cannot reduce the amount of dialysis since the dewatering could not be done either way. It also indicates that the suspensions have to be dialyzed until the conductivity becomes lower than 4.4 mS/cm for the electric field strengths used in this study.

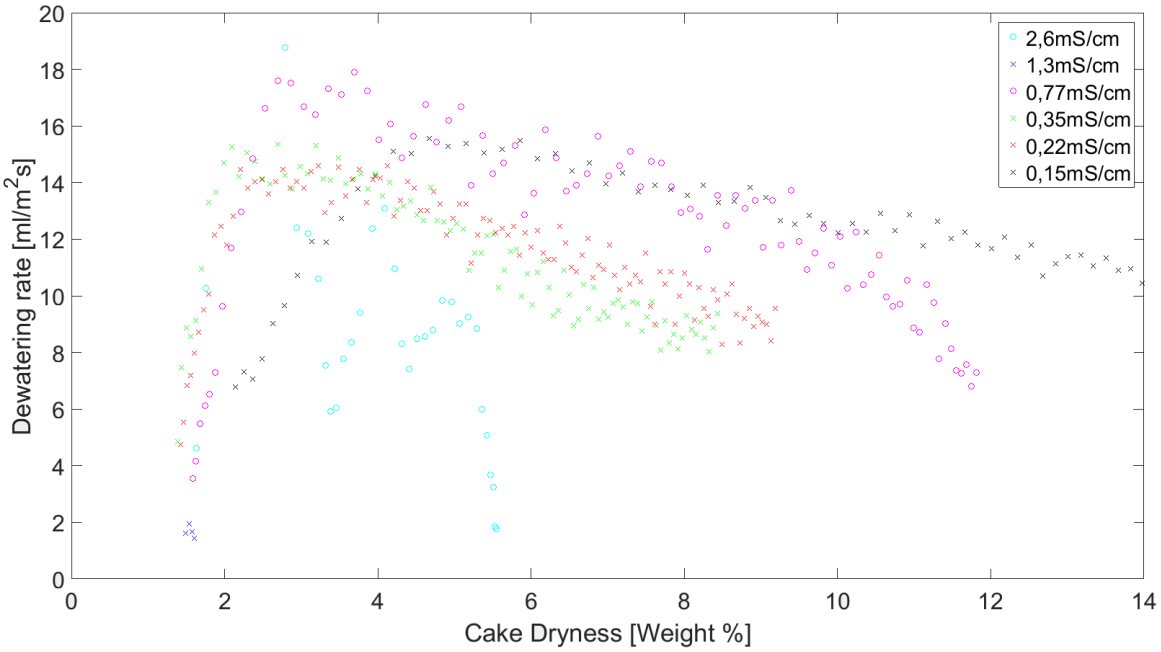

Figure 18. Dewatering rate during experiments with constant applied voltage of 5 V/cm for suspensions of cellulose nanocrystals at pH 5 with various electrical conductivities.

4.2.3.2.2 Specific energy demand

When looking at the energy demand for the different conductivity levels at different pH, see Figure 19, the dewatering experiments without pyrolysis were all in the same order of magnitude. The most dialyzed suspension had the lowest energy demand even if the difference was small, while the other suspensions were almost identical to each other. The energy demand for the suspensions where pyrolysis reactions occurred were excluded from the graph since the energy demand increased with an order of magnitude, see Figure 20.

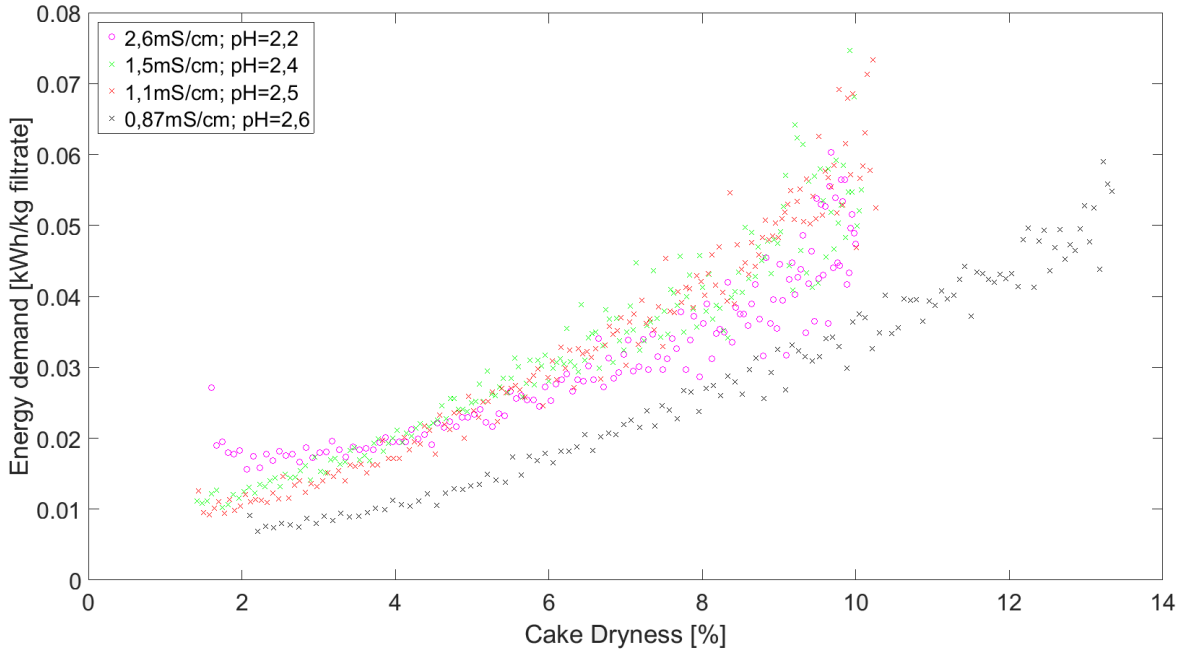

Figure 19. Energy demand during dewatering experiment with constant applied voltage of 5 V/cm for all successful suspensions at different pH.

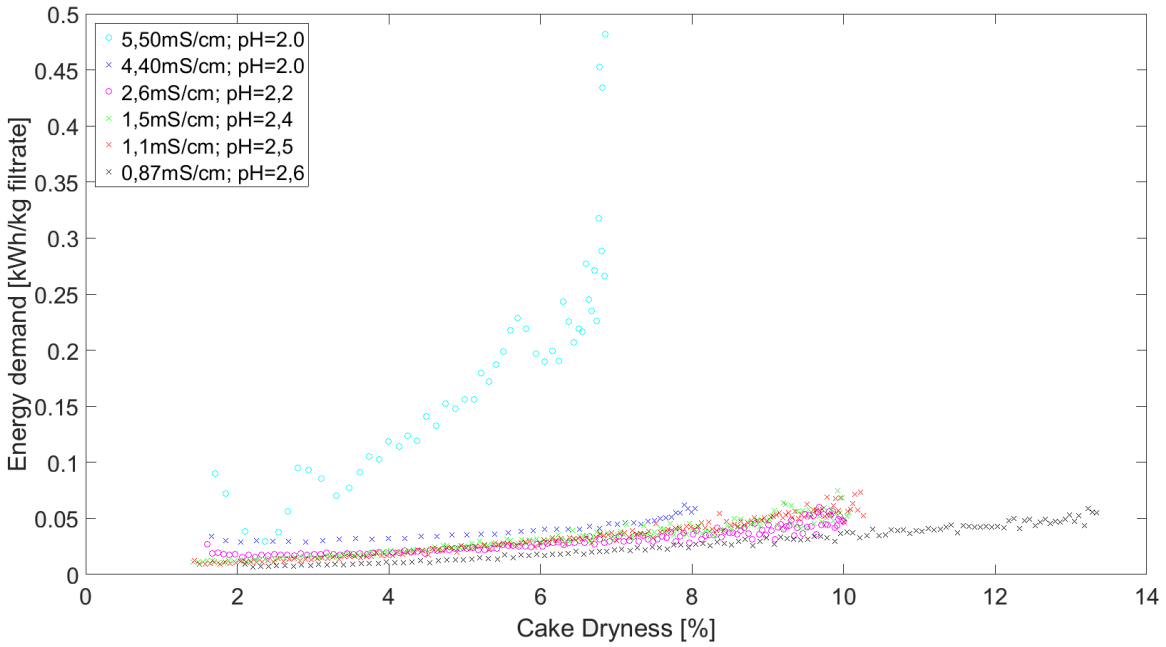

Figure 20. Energy demand during dewatering experiment with constant applied voltage of 5 V/cm for all suspensions at different pH.

The specific energy demand for suspensions with pH adjusted to 5 is given in Figure 21. Same trends could be seen for the suspensions with pH adjustment as for those without pH adjustment. Therefore the suspensions with initial conductivity of 2.6 mS/cm and 1.3 mS/cm were excluded from the graph since their energy demand increased with the same order of magnitude as for the suspensions without pH adjustment. The suspensions with lower electrical conductivities were all in the same magnitude of energy demand. With the

exception of the upstart of the experiment with 0.77 mS/cm which had significantly higher energy demand as a result of the low registered flow rate in the beginning of the experiment. However, the more dialyzed a suspension were, the lower the energy demand became.

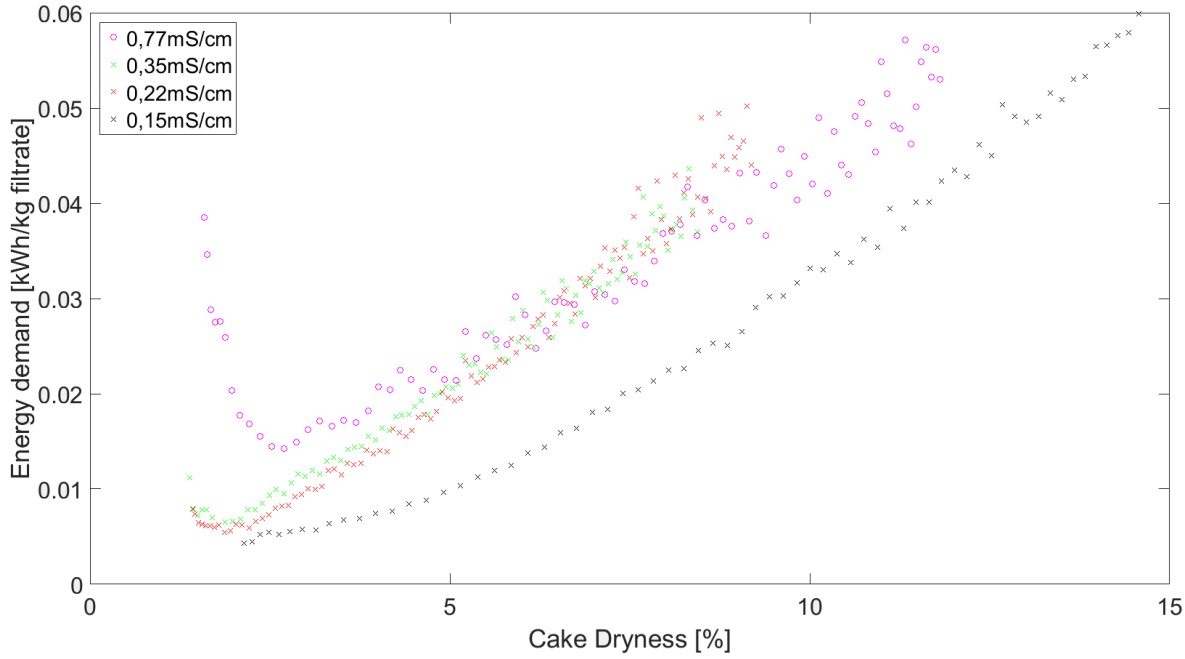

Figure 21. Energy demand during dewatering experiment with constant applied voltage of 5 V/cm for all successful suspensions at pH 5.

When looking at the energy demand of using electroosmotic dewatering it was evident that the energy demand varies from below 0.01 kWh/kg water removed to approximately 0.08 kWh/kg water depending on the solid content, how far the suspension was dialyzed and which pH the suspension had for the suspension with a constant applied voltage of 5 V/cm. For constant applied current of 0.3 A the energy demand was as high as 0.16 kWh/kg. Comparing this to the heat of vaporization for water, 0.63 kWh/kg (2260kJ/kg), shows that electroosmotic dewatering is potentially much more energy efficient for the electrical field strengths used in this study. As long as the dialysis is performed so that no pyrolysis reactions occur during the electroosmotic dewatering the operation of electroosmotic dewatering can be made energy efficient compared to drying. However, pyrolysis reactions can possibly be avoided by lowering the strength of the electric field to below 5 V/cm which could reduce the amount of time the dialysis have to be performed on the suspensions or the electric field could be set to above 5 V/cm if the suspensions are dialyzed far enough.

5 Conclusions

- Electroosmotic dewatering of cellulose nanocrystals was performed at a fraction of the energy demand of thermal drying from an initial solid content between 1.5- 2.0 weight % up to 10- 14 weight %.
- A lower conductivity of the suspension improves the energy efficiency of the electroosmotic dewatering operation. The lower the conductivity becomes, the less effect by further dialysis is achieved since the conductivity increased during the experiments.
- The suspensions of cellulose nanocrystals have to be dialyzed until the conductivity is at 8.5 mS/cm or lower otherwise the particles will not be fully dispersed during the sonication. For the electric field strengths used in this study the cellulose nanocrystals have to be dialyzed below 4.4 mS/cm or pyrolysis reactions occurred at the anode.
- The energy demand of the electroosmotic dewatering can be improved by pH adjustment of the suspension of cellulose nanocrystals. However, this affect is counteracted by electrolysis reactions at the anode lowering the pH in the throughout the dewatering operation.

6 Future work

Even though the experiments using electroosmotic dewatering were successful there is still work left to be done before industrial implementation. To see how the dewatering behaves at a larger scale is of outmost importance. How does the larger scale affect the energy demand and how much water can be removed per hour? Or will there be an area in the filter cell that is not used? Is there an increasing risk for pyrolysis reactions closer to the source of the electric field? These are just a few questions that would need answering before a large scale production can be made.

However there are even more things that could be tested that are of great importance, for example how dry can the filter cake become before it becomes impossible or impractically to dewatering it more this way without irreversibly affecting the particle properties? Or will the energy demand become too high before the dewatering rate goes down?

It could also be interesting to study different designs of filtration equipment, for example if there is possible to make a design where the electrolysis reactions are counteracted or the products from the electrolysis reactions are removed. This could improve the dewatering behavior as the pH adjusted suspensions both appeared with higher dewatering rate and less energy demand during the experiments.

Another thing that could be tested and analyzed is how the dewatering is affected by usage of another filter. In this study a filter of high quality is used to retain the solid particles. However, since the particles are repelled by the cathode a filter of lesser quality might could be used to lower the operation cost and the repelling effect of the electrophoresis might be enough to retain the particles completely which would mean that the filter only have to let the water move and not to retain the particles.

7 References

ABITBOL, T., RIVKIN, A., CAO, Y., NEVO, Y., ABRAHAM, E., BEN-SHALOM, T., LAPIDOT, S. & SHOSEYOV, O. 2016. Nanocellulose, a tiny fiber with huge applications. *Current Opinion in Biotechnology,* 39**,** 76-88.

ADAMSON, A. W. 1979. CHAPTER TWELVE - SOLUTIONS OF ELECTROLYTES. *In:* ADAMSON, A. W. (ed.) *A Textbook of Physical Chemistry (Second Edition).* Academic Press.

ATKINS, P. & JONES, L. 2010. *CHEMICAL PRINCIPLES THE QUEST FORINSIGHT* Clansy Marchal.

BÖRJESSON, M., SAHLIN, K., BERNIN, D. & WESTMAN, G. 2018. Increased thermal stability of nanocellulose composites by functionalization of the sulfate groups on cellulose nanocrystals with azetidinium ions. *Journal of Applied Polymer Science,* 135**,** 45963.

BÖRJESSON, M. & WESTMAN, G. 2015. Crystalline Nanocellulose — Preparation, Modification, and Properties. *In:* POLETTO, M. & JUNIOR, H. L. O. (eds.) *Cellulose - Fundamental Aspects and Current Trends.* Rijeka: InTech.

CARMAN, P. 1937. Fluid flow through granular beds. Transactions of the Institution of Chemical Engineers. 15**,** 150-166.

CURVERS, D., MAES, K. C., SAVEYN, H., DE BAETS, B., MILLER, S. & VAN DER MEEREN, P. 2007. Modelling the electro-osmotically enhanced pressure dewatering of activated sludge. *Chemical Engineering Science,* 62**,** 2267-2276.

DARCY, H. 1856. Les fontaines de publiques de la ville de Dijon. *Victor Dalamont, Paris*.

DELGADO, A. V., GONZÁLEZ-CABALLERO, F., HUNTER, R. J., KOOPAL, L. K. & LYKLEMA, J. 2007. Measurement and interpretation of electrokinetic phenomena. *Journal of Colloid and Interface Science,* 309**,** 194-224.

DUFRESNE, A. 2012. Nanocellulose - From Nature to High Performance Tailored Materials. De Gruyter.

HASANI, M., CRANSTON, E. D., WESTMAN, G. & GRAY, D. G. 2008. Cationic surface functionalization of cellulose nanocrystals. *Soft Matter,* 4**,** 2238-2244.

HENRIKSSON, G., BRÄNNVALL, E. & LENNHOLM, H. 2009. 2. The Trees. *Wood Chemistry and Wood Biotechnology*.

HENRIKSSON, G. & LENNHOLM, H. 2009. 4. Cellulose and Carbohydrate Chemistry. *Wood Chemistry and Wood Biotechnology.*

HIEMENZ, P. C. & RAJAGOPALAN, R. 1997. *Principles of colloid and surface chemistry, revised and expanded,* New York, CRC Press.

KOZENY, J. 1927. Über kapillare leitung des wassers im boden. Mathematisch-Naturwissenschaftliche. 136**,** 271–306.

LARUE, O. & VOROBIEV, E. 2004. Sedimentation and water electrolysis effects in electrofiltration of kaolin suspension. *AIChE Journal,* 50**,** 3120-3133.

LOGINOV, M., CITEAU, M., LEBOVKA, N. & VOROBIEV, E. 2013. Electro-dewatering of drilling sludge with liming and electrode heating. *Separation and Purification Technology,* 104**,** 89-99.

LYKLEMA, J. 1995. 4 - Electrokinetics and Related Phenomena. *In:* LYKLEMA, J. (ed.) *Fundamentals of Interface and Colloid Science.* Academic Press.

MAHMOUD, A., OLIVIER, J., VAXELAIRE, J. & HOADLEY, A. F. A. 2010. Electrical field: A historical review of its application and contributions in wastewater sludge dewatering. *Water Research,* 44**,** 2381-2407.

MOBERG, T., SAHLIN, K., YAO, K., GENG, S., WESTMAN, G., ZHOU, Q., OKSMAN, K. & RIGDAHL, M. 2017. Rheological properties of nanocellulose suspensions:

effects of fibril/particle dimensions and surface characteristics. *Cellulose,* 24**,** 2499-2510.

PENG, B. L., DHAR, N., LIU, H. L. & TAM, K. C. 2011. Chemistry and applications of nanocrystalline cellulose and its derivatives: A nanotechnology perspective. *The Canadian Journal of Chemical Engineering,* 89**,** 1191-1206.

RAGAUSKAS, A. J., WILLIAMS, C. K., DAVISON, B. H., BRITOVSEK, G., CAIRNEY, J., ECKERT, C. A., FREDERICK, W. J., HALLETT, J. P., LEAK, D. J., LIOTTA, C. L., MIELENZ, J. R., MURPHY, R., TEMPLER, R. & TSCHAPLINSKI, T. 2006. The Path Forward for Biofuels and Biomaterials. *Science,* 311**,** 484-489.

RUTH, B. F. 1935. Studies in Filtration III. Derivation of General Filtration Equations. *Industrial & Engineering Chemistry,* 27**,** 708-723.

SAHLIN, K., FORSGREN, L., MOBERG, T., BERNIN, D., RIGDAHL, M. & WESTMAN, G. 2018. Surface treatment of cellulose nanocrystals (CNC): effects on dispersion rheology. *Cellulose,* 25**,** 331-345.

SHIRATO, M., SAMBUICHI, M., KATO, H. & ARAGAKI, T. 1969. Internal flow mechanism in filter cakes. *AIChE Journal,* 15**,** 405-409.

WETTERLING, J. 2017. *Filtration of Microcrystaline Cellulose,* Gothenburg, Sweden, Chalmers University of Technology.

WETTERLING, J., JONSSON, S., MATTSSON, T. & THELIANDER, H. 2017a. The Influence of Ionic Strength on the Electroassisted Filtration of Microcrystalline Cellulose. *Industrial & Engineering Chemistry Research,* 56**,** 12789-12798.

WETTERLING, J., MATTSSON, T. & THELIANDER, H. 2017b. Local filtration properties of microcrystalline cellulose: Influence of an electric field. *Chemical Engineering Science,* 171**,** 368-378.

WETTERLING, J., SAHLIN, K., MATTSSON, T., WESTMAN, G. & THELIANDER, H. 2018. Electroosmotic dewatering of cellulose nanocrystals. *Cellulose,* 25**,** 2321-2329.